

## Experimental Analysis of Heat Transfer Distribution in the Passive Residual Heat Removal System of SMART-ITL

Yu-Na Kim<sup>a\*</sup>, Jin-Hwa Yang<sup>a</sup>, Hwang Bae<sup>a</sup>, Sung-Uk Ryu<sup>a</sup>, Byong Guk Jeon<sup>a</sup>, Eunkoo Yun<sup>a</sup>, Yun-Gon Bang<sup>a</sup>, Sung-Jae Yi<sup>a</sup>, Young In Kim<sup>a</sup>, Hyun-Sik Park<sup>a</sup>

<sup>a</sup>Korea Atomic Energy Research Institute, 989-111 Daedeokdaero, Yuseong, Daejeon, 305-353, Korea

\*Corresponding author: ynkim@kaeri.re.kr

### 1. Introduction

SMART, which is an integral small modular reactor designed by KAERI (Korea Atomic Energy Research Institute), has passive safety systems based on the design characteristics of inherent safety [1]. Among them, the PRHRS (Passive Residual Heat Removal System) removes the RCS (Reactor Coolant System) heat by natural circulation in emergency situations where the cooling by secondary system is not available. Since the PRHRS involves complex thermal hydrodynamic phenomena such as condensation and boiling heat transfer during natural circulation, it is difficult to accurately predict the heat removal capability. Therefore, the performance verification test using the integral-effect test facility, called SMART-ITL, was performed. In order to estimate the heat removal performance of the prototypical PRHRS based on the experimental results from the scale-down facility, it is necessary to distinguish the heat transfer rate of the heat exchanger from the total heat transfer rate. Therefore, this paper analyzed the heat transfer distribution in the PRHRS loop during the performance verification test to divide the heat transfer rate throughout each section.

### 2. PRHRS performance verification test

#### 2.1. Facility

SMART-ITL facility is an integral effect test facility to simulate the primary and secondary system as well as passive safety systems of SMART [2]. The primary system was designed to operate under the same conditions as SMART, which is that the core exit temperature and pressurizer pressure are 323 °C and 15 MPa, respectively. Its height is preserved to the full scale, and its area and volume are scaled down to 1/49 compared with the prototype plant. The full height scale is important to preserve the thermal-hydraulic characteristics in some phenomena, the natural circulation in particular, such as PRHRS. The PRHRS consists of four trains, each of which is composed of a heat exchanger (HX) in an emergency cool-down tank (ECT), a makeup tank (MT) and connecting pipes. The diameter, thickness, pitch and orientation of the heat exchanger tube are same as those of SMART, while the number of tubes was reduced to 1/49, in order to reveal the heat removal capacity of a single tube [3].

#### 2.2. Test condition

These tests were conducted to investigate the heat transfer distribution of PRHRS. Thus, the steady-state conditions of the primary and secondary sides with operating PRHRSs were observed, while maintaining the core exit temperature of primary side constant. Two experiments, Test 1 and Test 2, were conducted with different RCS temperature, and the temperature of Test 1 is higher than Test 2. Since the coolant temperature of the ECT is also maintained at the saturation temperature, the ECT water level gradually decreases with evaporation during PRHRS operation. The experimental data includes the local temperature, pressure and flow rate at the locations indicated in Fig. 1.

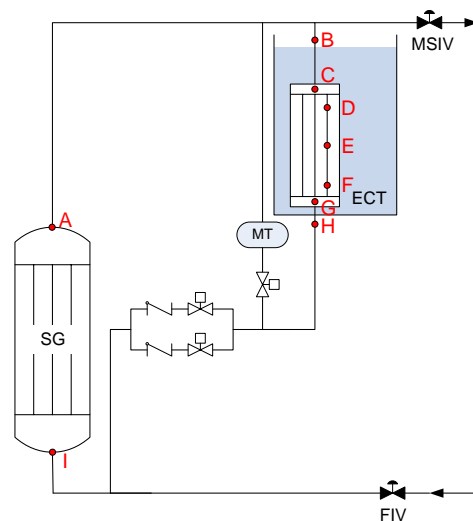


Fig. 1 Schematics of the test facility for SMART PRHRS

#### 2.3. Experimental results

Fig. 2 shows the temperature distribution of the PRHRS loop. The superheated steam discharged from the steam generator outlet gradually decreases in temperature as it flows along the piping, and when it reaches the saturation temperature, it condenses while maintaining the temperature. Therefore, it can be estimated that the void fraction is gradually decreasing even if the temperature does not change in the saturation region. After the vapor is completely condensed, the temperature starts to reduce rapidly.

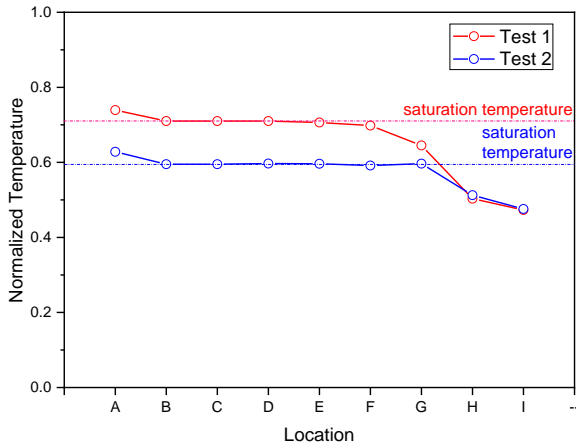


Fig. 2 Temperature distribution of the secondary system

### 3. Heat transfer distribution analysis

Heat transfer could occur throughout the PRHRS loop, including the pipes overlaid with insulator. In order to distinguish the independent heat removal capability of the PRHRS heat exchanger, heat transfer distribution in the loop should be analyzed. The heat transfer rate for each section was calculated by the following procedures using the experimental data as much as possible.

#### 3.1. Section H-I (Insulated pipes from ECT outlet to SG inlet)

The heat transfer rate can be simply estimated by heat transfer equation based on the theoretical thermal conductivity of the pipe and insulator materials, stainless steel and perlite, respectively. The conductivity of stainless steel was determined by the ambient fluid temperature [4]. However, it is not possible to assume that the insulation is complete due to the realistic limitations. Therefore, using the temperature and pressure data in Section H-I, we calculated the actual thermal conductivity of the insulator as follows:

$$Q = \frac{(T_{\infty 1} - T_{\infty 2})}{\frac{1}{2\pi r_1 L h_{in}} + \frac{\ln(r_2 / r_1)}{2\pi L k_{stain}} + \frac{\ln(r_3 / r_2)}{2\pi L k_{insul}} + \frac{1}{2\pi r_3 L h_{out}}} \quad (1)$$

where  $r_1$ ,  $r_2$ ,  $r_3$  are the inner and outer radiuses of pipe and outer radius of insulator, respectively.  $Q$ ,  $h$ ,  $k$  and  $L$  mean heat transfer rate, convective heat transfer coefficient, conductivity and length of pipe, while  $T_{\infty 1}$  and  $T_{\infty 2}$  stand for the temperatures of inner and outer fluids.

The thermal resistances by inner and outer convection are neglected since these effects are much smaller than insulator, so only those of pipe and insulator are considered. The heat transfer rate can also be estimated

by the enthalpy change of the coolant as expressed by Equation (2).

$$Q = \dot{m}(H_H - H_I) \quad (2)$$

$\dot{m}$  and  $H$  stand for the mass flow rate and enthalpy, respectively. Thus, the actual thermal conductivity of insulator can be deduced by comparing the two calculated heat transfer rates. As a result, it is calculated to be 0.12 which is greater than the theoretical value of 0.05.

#### 3.2. Section A-B (Insulated pipes from SG outlet to ECT inlet)

The heat transfer rate of Section A-B could be determined by Equation (1) with the previously deduced thermal conductivity of insulator. After the calculation, in order to identify the heat conservation, it was confirmed that the heat transferred from steam generator except the heat loss in Sections A-B and H-I is equal to the heat transferred to ECT which is calculated based on ECT water level change.

#### 3.3. Sections D-E-F (A heat exchanger tube)

The heat transfer rate through the heat exchanger tube can be inferred from the thermal conduction through the stainless steel tube which could be calculated by the measured temperatures of inside and outside wall, represented as  $T_{w,in}$  and  $T_{w,out}$ , respectively.

$$Q = 2\pi L k_{stain} \frac{(T_{w,in} - T_{w,out})}{\ln(r_2 / r_1)} \quad (3)$$

The condensation heat transfer rate on the inside wall and the boiling heat transfer rate on the outside wall should be equal to the conduction heat transfer rate. The estimated condensation and boiling heat transfer coefficients are reasonable values from 5,000 to 16,000 W/m<sup>2</sup>-K, and it was indicated that those tend to decrease with decreasing the void fraction.

#### 3.4. Sections B-C and G-H (Submerged pipes in ECT)

The heat transfer rates through the pipes submerged in ECT coolant are evaluated based on the estimated condensation and boiling heat transfer coefficients, represented as  $h_{cond}$  and  $h_{boil}$ , respectively. Assuming that the difference of heat transfer coefficient, derived by change of void fraction between the submerged pipes and the heat exchanger tubes, is negligible, the Section B-C adopts the heat transfer coefficients of the Location D, while the Section G-H uses that of the Location F. Actually, it is reasonable assumption for Test 1, since the phase of coolant is probably subcooled water both at

Location F and Section G-H. However, in the case of Test 2, the phase of coolant at Location F is estimated as saturated mixture, while Section G-H is subcooled mixture. Adopting the assumption to Test 2, the result is somewhat uncertain, but there are no other applicable estimations. This limit will improve in the future. Total thermal resistance including the convective terms is defined as denominator of Equation (4).

$$Q = \frac{(T_{\infty 1} - T_{\infty 2})}{\frac{1}{2\pi r_1 L h_{cond}} + \frac{\ln(r_2/r_1)}{2\pi L k_{stain}} + \frac{1}{2\pi r_2 L h_{boil}}} \quad (4)$$

### 3.5. Sections C-D and F-G (Heat exchanger headers)

The header of the PRHRS heat exchanger has a complicated structure, which makes it difficult to simply predict the heat transfer capacity. Instead, it can be assessed by subtracting the heat transfer rates in all sections except the header from total heat transfer rate.

## 4. Results and conclusions

Table 1 represents the results of calculation for the heat transfer distribution in PRHRS. As a result, approximately 40% of the total heat transfer rate in PRHRS loop of SMART-ITL occurs in two heat exchanger tubes, and the headers have heat removal capability for a single heat exchanger tube. In addition, about 10% of the heat is released by the heat loss of the insulated pipes, and about 30% is removed from the submerged pipes in the ECT. This distribution was not significantly different even if the RCS temperature was different, but in Test 2, when the RCS temperature was lower than Test 1, the heat transfers in the lower header and the lower submerged pipe is more enhanced than Test 1, because condensation did not occur completely in the heat exchanger.

Table 1 Calculation results for the heat transfer distribution in PRHRS

Section	Normalized heat transfer rate (Individual rate/ Total rate, %)	
	Test 1	Test 2
A-B	5.8	5.7
B-C	21.8	18.8
C-D and F-G	20.1	24.4
D-E-F	40.4	39.2
G-H	8.6	11.8
H-I	2.7	3.4

Figure 2 shows the change in fluid enthalpy and void fraction of test1 estimated based on the thermal distribution calculation. The enthalpy is calculated based on the Point F where the coolant is subcooled. The smaller the void fraction, the more gradually the condensation heat transfer becomes inactive and the lower the enthalpy reduction rate. On the other hand, superheated steam emitted from the steam generator was found to be completely condensed before the outlet of the heat exchanger tube.

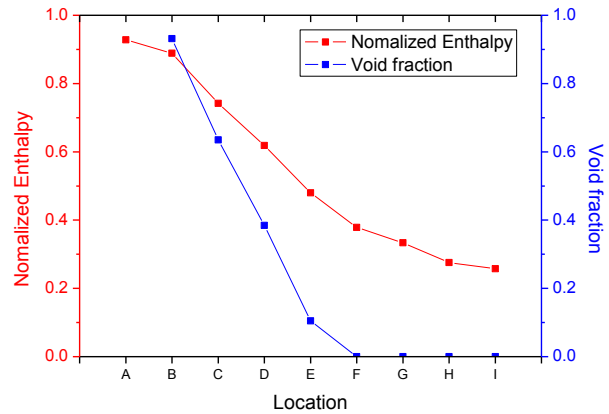


Fig. 2 Variation of enthalpy and void fraction (Test 1)

It is also possible to estimate the condensation heat transfer coefficient at each point in the heat exchanger tube section where the wall temperatures were measured. These values can be used to determine the appropriateness of the condensation heat transfer model. Figure 3 shows the result of comparison between the heat transfer coefficients estimated by experimental data and calculated using the Dittus-Boelter equation, which is a representative model for heat transfer in a pipe. As a result, the heat transfer coefficient difference between the model and the experiment increased as the condensation heat transfer became dominant. This means that the heat removal performance of the PRHRS can be overestimated if the model is used. Therefore, it is necessary to use another model or to check whether the error is within acceptable range through conservative assumptions.

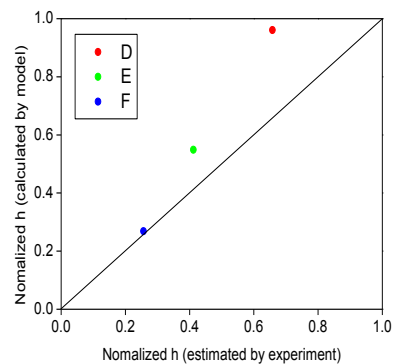


Figure 3 Comparison of heat transfer coefficients (Test 1)

## **5. Conclusion**

The heat transfer distribution of the PRHRS loop was obtained by using temperature and pressure data obtained from the experiment. As a result, the heat transferred through the heat exchanger tube was about 40% of the total heat removal, and it was analyzed that significant heat transfer occurred in the section where condensation heat transfer occurs, such as the upper pipe and header in ECT. Therefore, in order to calculate PRHRS heat removal performance more precisely, it is necessary to consider the heat transfer in these additional structures, and appropriate condensation heat transfer model should be selected using the given experimental data.

## **Acknowledgments**

This work was supported by the National Research Foundation of Korea (NRF) grant funded by the Korea government (MSIT). (No. 2016M2C6A1004894)

## **REFERENCES**

- [1] K. K. Kim, W. J. Lee, et al., SMART: The First Licensed Advanced Integral Reactor, *Journal of Energy and Power Engineering*, 8, pp.94-102, 2014.
- [2] H.S. Park, S.J. Yi, C.H. Song, SMR accident simulation in experimental test loop, *Nuclear Engineering International*, pp. 12-15, 2013.
- [3] H. Bae, D. E. Kim, et *al.*, Test facility design for the validation of SMART passive safety system, *Transactions of the Korean Nuclear Society Spring Meeting*, May 30-31, 2013, Gwangju, Korea.
- [4] SWEET, J. N., ROTH, E. P., MOSS, M., Thermal conductivity of Inconel 718 and 304 stainless steel, *International Journal of Thermophysics*, 8.5, pp.593-606, 1987.